Snapshots of Catalysis: the Structure of Fructose-1,6-(bis)phosphate Aldolase Covalently Bound to the Substrate Dihydroxyacetone Phosphate[†,‡]

Kyung H. Choi,[§,||] Jun Shi,[||] Christopher E. Hopkins,[§] Dean R. Tolan,*[,§] and Karen N. Allen*[,||]

Department of Biology, Boston University, 5 Cummington Street, Boston, Massachusetts 02215, and Department of Physiology and Biophysics, Boston University School of Medicine, 80 East Concord Street, Boston, Massachusetts 02118-2394

Received July 17, 2001; Revised Manuscript Received September 17, 2001

ABSTRACT: Fructose-1,6-bis(phosphate) aldolase is an essential glycolytic enzyme found in all vertebrates and higher plants that catalyzes the cleavage of fructose 1,6-bis(phosphate) (Fru-1,6-P_2) to glyceraldehyde 3-phosphate and dihydroxyacetone phosphate (DHAP). Mutations in the aldolase genes in humans cause hemolytic anemia and hereditary fructose intolerance. The structure of the aldolase−DHAP Schiff base has been determined by X-ray crystallography to 2.6 Å resolution ($R_{cryst} = 0.213$, $R_{free} = 0.249$) by trapping the catalytic intermediate with $NaBH_4$ in the presence of Fru-1,6-P_2. This is the first structure of a trapped covalent intermediate for this essential glycolytic enzyme. The structure allows the elucidation of a comprehensive catalytic mechanism and identification of a conserved chemical motif in Schiff-base aldolases. The position of the bound DHAP relative to Asp33 is consistent with a role for Asp33 in deprotonation of the C4-hydroxyl leading to C−C bond cleavage. The methyl side chain of Ala31 is positioned directly opposite the C3-hydroxyl, sterically favoring the *S*-configuration of the substrate at this carbon. The "trigger" residue Arg303, which binds the substrate C6-phosphate group, is a ligand to the phosphate group of DHAP. The observed movement of the ligand between substrate and product phosphates may provide a structural link between the substrate cleavage and the conformational change in the C-terminus associated with product release. The position of Glu187 in relation to the DHAP Schiff base is consistent with a role for the residue in protonation of the hydroxyl group of the carbinolamine in the dehydration step, catalyzing Schiff-base formation. The overlay of the aldolase−DHAP structure with that of the covalent enzyme−dihydroxyacetone structure of the mechanistically similar transaldolase and KDPG aldolase allows the identification of a conserved Lys-Glu dyad involved in Schiff-base formation and breakdown. The overlay highlights the fact that Lys146 in aldolase is replaced in transaldolase with Asn35. The substitution in transaldolase stabilizes the enamine intermediate required for the attack of the second aldose substrate, changing the chemistry from aldolase to transaldolase.

Fructose-1,6-bis(phosphate) aldolases [D-fructose 1,6-bis-(phosphate):D-glyceraldehyde 3-phosphate lyase, EC 4.1.2.13] are ubiquitous glycolytic enzymes that catalyze the reversible cleavage of fructose 1,6-bis(phosphate) (Fru-1,6-P_2)[1] to the triose phosphates glyceraldehyde 3-phosphate (G3P) and dihydroxyacetone phosphate (DHAP). The aldolases are categorized into two classes depending on their chemical mechanisms (*1*). The class I aldolases of animals and higher plants utilize covalent catalysis through a Schiff base formed between a lysine residue of the enzyme and ketose substrates. The class II aldolases of most bacteria and fungi require a divalent metal cation as a cofactor to polarize the ketose carbonyl oxygen (*2*). Among the class I enzymes found in vertebrates, there are three tissue-specific aldolases: aldolase A (found in skeletal muscle and red blood cells), aldolase B (found in liver, kidney, and small intestine), and aldolase C (found in neuronal tissues and smooth muscle) (*3*, *4*). In fructose metabolism, fructose 1-phosphate (Fru-1-P) is a substrate and aldolase isozymes have different activities for Fru-1,6-P_2 and Fru-1-P (*5*). This differential activity has been used as a basis for discriminating among these isozymes in tissues and in the diagnosis of a variety of disease states such as liver damage, cancer, and hereditary fructose intolerance (*6*−*8*). The structural differences between these isozymes, which could explain the kinetic differences, are unknown. An understanding of the mechanisms by which the aldolase isozymes catalyze their respective reactions

[†] This work has been supported by grants from the NIH to D.R.T. (DK-43521 and GM-60616) and K.N.A. (GM-60616). Use of the Advanced Photon Source was supported by the U.S. Department of Energy, Basic Energy Sciences, Office of Science, under Contract W-31-109-Eng-38. Use of the BioCARS Sector 14 was supported by the National Institutes of Health, National Center for Research Resources, under Grant RR07707.

[‡] The coordinates have been deposited with the Protein Data Bank (entry 1J4E) and are also available from the corresponding authors upon request.

* To whom correspondence should be addressed. D.R.T.: Biology Department, Boston University, 5 Cummington St., Boston, MA 02215; phone, (617) 353-5310; fax, (617) 353-6340; e-mail, tolan@bu.edu. K.N.A.: Department of Physiology and Biophysics, Boston University School of Medicine, 80 E. Concord St., Boston, MA 02118-2394; phone, (617) 638-4398; fax, (617) 638-4273; e-mail, allen@med-xtal.bu.edu.

[§] Boston University.

[||] Boston University School of Medicine.

[1] Abbreviations: DHAP, dihydroxyacetone phosphate; Fru-1-P, fructose 1-phosphate; Fru-1,6-P_2, fructose 1,6-bis(phosphate); G3P, glyceraldehyde 3-phosphate; KDPG aldolase, 2-keto-3-deoxy-6-phosphogluconate aldolase; rms, root-mean-square.

10.1021/bi0114877 CCC: $20.00
Published on Web 10/26/2001

could be the key to the treatment of the diseases caused by aldolases such as hemolytic anemia and hereditary fructose intolerance.

The catalytic mechanism has been extensively studied using class I aldolase A from rabbit muscle, which differs by seven amino acids from that of humans, and can be considered for all intents and purposes identical with the human muscle enzyme (*9*, *10*). It is clear that aldolase cleavage proceeds through a number of distinct enzyme−substrate intermediates, including carbinolamine, imine (Schiff base), and an enamine/carbanion (*11*−*14*). A lysine residue in the active site of aldolase attacks the carbonyl carbon of the substrate, leading to the formation of a carbinolamine followed by dehydration to form a Schiff base (*11*, *15*). Subsequent cleavage of the C3−C4 bond releases G3P and leaves an enamine/carbanion at the active site (*12*, *16*). Protonation of the carbanion and hydrolysis of the resultant Schiff base release the second product DHAP, regenerating the enzyme (*14*). With the exception of the Schiff base forming Lys229 (*17*), the role of essential amino acid residues in the active site is equivocal or completely unknown (*18*−*21*). The assignment of a role for each residue in the active site has been hampered, even after several liganded structures were determined, by inconsistent binding modes for the ligands or nonproductive binding (*22*−*24*). For example, in the DHAP-complexed structure, the ligand was localized in three alternate conformations showing three different interactions with the enzyme (*24*).

As a step toward understanding the catalytic mechanism in atomic detail, we have trapped a Schiff-base intermediate complex of Fru-1,6-P_2 aldolase A by reduction with borohydride, and we report herein the structure of this complex. This is the first covalent intermediate structure reported for this important glycolytic enzyme. The structure reveals residues involved in substrate binding and clarifies the functional roles involved in each step of catalysis. Furthermore, when compared to the structures of transaldolase (*25*) and 2-keto-3-deoxy-6-phosphogluconate (KDPG) aldolase (*26*), the structure suggests a common chemical motif, namely, a Lys-Glu dyad for class I aldolase chemistry.

MATERIALS AND METHODS

Materials. Glycerol-3-phosphate dehydrogenase/triose phosphate isomerase was purchased from Boehringer Mannheim. Fru-1,6-P_2, $NaBH_4$, and other chemicals were from Sigma Chemical Co. or Fluka. Cm-Sepharose CL-6B Fast Flow was from Pharmacia. Oligonucleotides for site-directed mutagenesis and sequence determination were synthesized on Milligen/Biosearch DNA synthesizers using phosphoramidite chemistry or purchased from Midland, Inc.

Purification of Aldolase. Site-directed mutagenesis of pPB14 (*19*) was performed by modification of the overlap-extension PCR method as reviewed by Ling and Robinson (*27*). Four surface cysteines (C72, C239, C289, and C338) were mutated to alanine residues. The recombinant protein was expressed and purified in the same manner as the wild type (C. E. Hopkins et al., personal communication). The protein was >95% pure as determined by SDS−PAGE (12%). Protein was precipitated with 70% saturated ammonium sulfate, and protein suspensions were stored at 4 °C until they were used.

Activity Assay. Protein concentrations were determined by absorbance at 280 nm using an E_{280}(0.1%) of 0.91 mg/mL (*28*). The activity of aldolase was determined in a coupled assay using glycerol-3-phosphate dehydrogenase/triose phosphate isomerase (*29*). Aldolase was diluted in 50 mM TEA-HCl (pH 7.4) and added to a cuvette containing 50 mM TEA-HCl (pH 7.4), 10 mM EDTA, 0.16 mM NADH, and 10 μg/mL glycerol-3-phosphate dehydrogenase/triose phosphate isomerase (10:1). The substrate cleavage rate was determined by measuring the decrease in absorbance per minute at 340 nm.

Sodium Borohydride Reduction of the Fru-1,6-P_2 Aldolase−Substrate Complex. The reduction of the Schiff-base intermediate by sodium borohydride was carried out on the basis of the procedures described previously by others (*30*) with some modification. Purified aldolase (61 μM, final concentration) was incubated in 200 μL of 50 mM HEPES buffer (pH 8.0) for 15 min with a 4-fold molar excess of Fru-1,6-P_2 (240 μM; 20K_m). Then 400 μL of 200 mM $NaBH_4$ in 200 mM MES buffer (pH 6.0) was added, and the pH was adjusted to 6.0 with acetic acid. An additional portion of Fru-1,6-P_2 and $NaBH_4$ solution was added after 15 min to ensure the completion of the reduction. After each addition, aliquots were removed and the activity of the enzyme was determined. The highest concentration of reductant that did not inactivate the enzyme after a single addition (200 mM $NaBH_4$) was used in the experiment, although this concentration caused some inactivation in the absence of substrate after a second addition of reductant (60% of control activity). After the reaction was judged to be 90−95% complete, the solution was concentrated to 10 mg/mL protein and the buffer was changed to 20 mM HEPES (pH 8.0) using an UltraFree centrifugal concentrator (Millipore) with a 10 kDa cutoff membrane.

Crystallization. Crystals of the borohydride-reduced protein were obtained using previously known conditions (*22*). Crystals were grown using hanging drop geometry and the vapor diffusion method. A protein concentration of 10 mg/mL was used. A drop (5 μL) of the protein solution was mixed with an equal volume of drop buffer consisting of 0.1 M Tris-HCl (pH 7.4), 0.1 mM DTT, 1 mM β-mercaptoethanol, 1 mM EDTA, and 10% PEG, and suspended over a well containing 0.1 M Tris-HCl (pH 7.4) and 28% PEG 6000. Crystals grew at 18 °C in 1 week in the form of thin plates with dimensions of 0.5 mm × 0.3 mm × 0.05 mm. 2-Methyl-2,4-pentanediol (20% final concentration) was added to the drop containing crystals immediately prior to data collection as a cryoprotectant.

Data Collection. Data were collected by freezing the cryoprotected crystal directly in a stream of nitrogen cooled to −180 °C at BM 14C at Argonne National Laboratory (Argonne, IL). A crystal-to-detector distance of 200 mm and 1° oscillations were used. The programs DENZO and SCALEPACK (*31*) were used to index and reduce the data, respectively. The space group is $P2_1$ with the following unit cell dimensions: $a = 82.8$ Å, $b = 100.6$ Å, $c = 84.5$ Å, and $\beta = 98.3°$. The assignment to $P2_1$ was made by assessing systematic absences. The data set, obtained from a single crystal, was 86% complete overall to 2.6 Å resolution with $I/\sigma = 10$ in the highest-resolution shell. The number of molecules in the asymmetric unit was calculated to be four, assuming a Matthews constant of 2.3 Å^3/Da (*32*).

Structure Determination, Refinement, and Model Building. The initial phase information was obtained by molecular replacement with the previously determined aldolase A structure [PDB entry 6ALD (*22*)] using CNS (*33*). The initial structural model gave a crystallographic *R*-factor of 0.28. For the calculation of R_{free} during the refinement, 10% of all reflections were excluded. Rigid-body refinement was performed in the program CNS, defining each monomer as a rigid body to refine the relative orientation of the monomers in the tetramer. Each round of refinement included rigid-body, positional, slow-cooling, and *B*-group refinement followed by manual rebuilding on a Silicon Graphics O2 workstation. NCS restraints with a high weight (300 kcal mol^{-1} $Å^{-2}$) were used throughout the refinement. The final model was examined with a composite omit map generated in CNS. In the final round of refinement, the model of covalently attached DHAP was added. Topology and parameter files for the DHAP-linked lysine were generated by the xplor2d program in the CCP4 program suite (*34*). Water molecules were added to the model using an $F_o - F_c$ map with electron density contoured at 3σ and a $2F_o - F_c$ map contoured at 1.0σ. The geometric parameters of the model were analyzed with PROCHECK. In addition, a working model of Fru-1,6-P_2 covalently bound at the active site was generated for the sole purpose of analyzing the protein groups proximal to C4. The model was produced in the molecular graphics program O (*35*) by substituting the pro-*S* hydrogen at C3 with the C4 carbon of Fru-1,6-P_2. The coordinates have been deposited with the Protein Data Bank (entry 1J4E) and are also available from the corresponding authors upon request.

RESULTS AND DISCUSSION

Generation of the gtet Mutant. Rabbit muscle aldolase contains eight cysteines per monomer. Four of these are located on the surface of the protein with the remaining four in the interior of the protein. Loss of activity by formation of disulfide bonds or reaction with sulfhydryl reagents has previously been observed in Fru-1,6-P_2 aldolase. Large variations in the activity of purified muscle aldolase after storage may relate to the oxidation of the surface cysteines. To improve crystallization by increasing the stability of the enzyme, four surface cysteines (C72, C239, C289, and C338) were mutated to Ala. The resulting protein exhibited the same activity as the wild type toward Fru-1,6-P_2 ($k_{cat} = 14 \pm 1$ s^{-1}, $K_m = 12 \pm 0.5$ μM) and was more stable in long-term storage at 25 °C than the wild type.

Borohydride Reduction of the Schiff-Base Intermediate. Incubation of aldolase with the substrate Fru-1,6-P_2 leads to the formation of an enzyme−Schiff-base intermediate (substrate Schiff base) which, after C−C bond cleavage, yields the product Schiff base. The Schiff-base intermediate trapped by borohydride reduction has been previously identified as N^6-(phosphoglyceryl)lysine or the product Schiff base (*30*). A 4-fold molar excess of Fru-1,6-P_2 over enzyme ($20K_m$) was used during incubation and borohydride reduction to saturate the active site with substrate. The loss of enzyme activity was monitored by a coupled assay (*29*) as the reduced enzyme−Schiff-base complex formed. After addition of two aliquots of substrate and $NaBH_4$, with a >2000-fold molar excess over the enzyme, only 8% of the activity remained. A single borohydride treatment of aldolase in the absence of the substrate, Fru-1,6-P_2, resulted in no inactivation. The enzyme complex reaction mixture was then extensively dialyzed to remove any unbound substrate or products from the protein.

Table 1: Data Collection and Refinement Statistics

data collection	
resolution (Å)	∞−2.6
no. of reflections	35634
completeness (overall/outer shell) (%)	86/60
R_{sym} (overall/outer shell)	0.034/0.220
I/σ (overall/outer shell)	20/10
refinement statistics	
no. of protein atoms (non-hydrogen)	10432
no. of water molecules	125
no. of hetero molecules	4
resolution (Å)	100−2.6
σ cutoff	0.0
R_{cryst}[a]	0.213
R_{free}[b]	0.249
mean *B*-factor ($Å^2$)	31.9
rms deviation	
bonds (Å)	0.008
angles (deg)	1.303
dihedrals (deg)	22.463
impropers (deg)	0.979

[a] $R = \sum[(I - \langle I \rangle)^2]/\sum I^2$. [b] R_{free} was calculated from a random selection constituting 10% of the data.

Structure Determination. The rabbit muscle aldolase A covalently linked to DHAP crystallized in space group $P2_1$ with four monomers in an asymmetric unit, consistent with the fact that the enzyme is a homotetramer in solution. The crystal structure was determined by molecular replacement (Table 1) and refined to 2.6 Å resolution. The final structure had an R_{cryst} of 0.213 and an R_{free} of 0.249 using data in the resolution range of 100−2.6 Å and no I/σ cutoff. The final structure contained residues 4−344, 125 water molecules, and four covalently linked DHAP molecules. The Ramachandran plot produced by PROCHECK shows that 91.7% of the residues are in the "favored" regions with the remaining 8.3% of the residues in the "allowed" region. No residue was found in either "generously allowed" or "disallowed" regions. The structure was well determined with an average *B*-factor of 31.9 $Å^2$ for both main chain and side chain atoms. The 19 C-terminal residues (345−363) were disordered and not included in the model. This C-terminal region of Fru-1,6-P_2 aldolase is involved in substrate specificity, based on the results of chemical modification, truncation, and site-directed mutagenesis experiments (*36*−*40*). The lack of ordered structure for the C-terminus of the protein is consistent with these findings.

The monomers comprising the tetramer are nearly identical to one another with a root-mean-square (rms) deviation of 0.03 Å. Both the tertiary structure of the monomer and the quaternary structure of the tetramer in the aldolase−Schiff-base complex are similar to those of native human aldolase (*23*, *41*), indicating that there is no large overall change in conformation upon substrate binding and catalysis. The rms deviation between the native human enzyme and this complex for the 341 common Cα atoms (excluding the first three residues and disordered C-terminus) was 0.346 Å. The protein structure is similar to that of rabbit aldolase A complexed noncovalently with DHAP (*24*) or Fru-1,6-P_2 (*22*) with rms deviations of 0.343 and 0.226 Å, respectively, for 341 common Cα atoms. Thus, with the possible exception

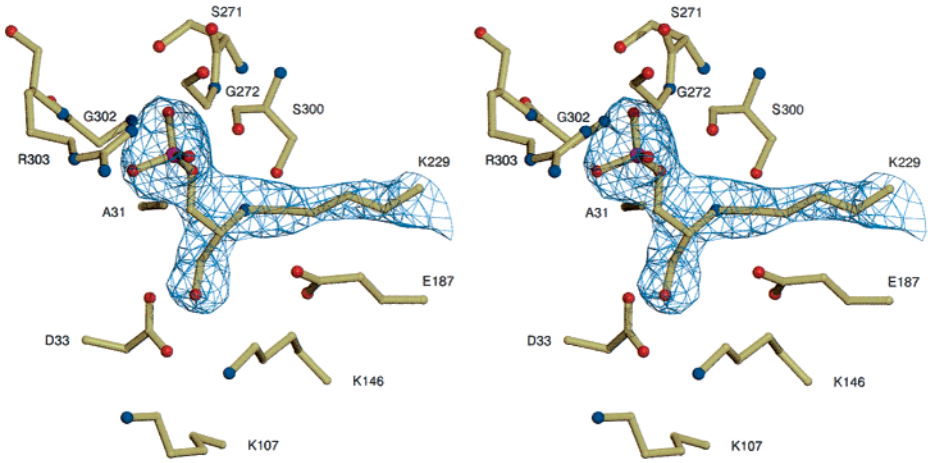

FIGURE 1: Stereoview of electron density showing the Schiff-base intermediate and the surrounding residues. The electron density from a $2F_o - F_c$ omit map (contoured at 1.0σ) is depicted in cyan, and residues are depicted as ball-and-stick models. The figure was generated using the program MOLSCRIPT (*60*) and POV-Ray (Persistence of Vision Ray Tracer, version 3.01).

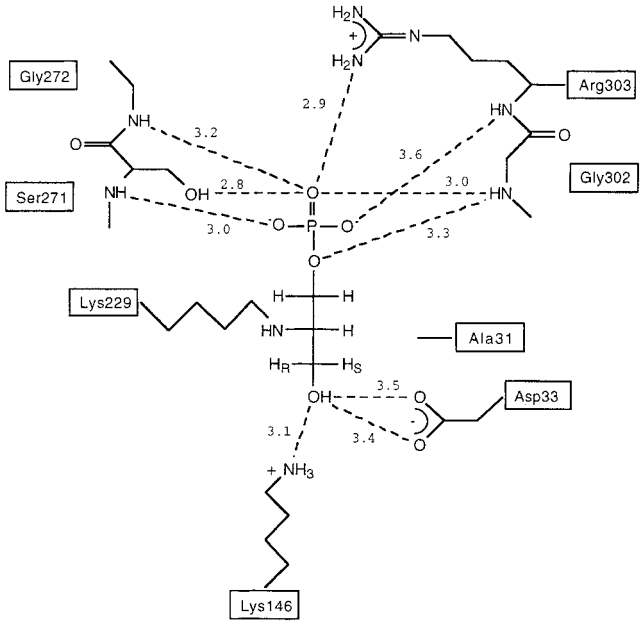

FIGURE 2: Schematic representation of the reduced Schiff-base intermediate with the surrounding residues at the active site. Putative hydrogen bonds between the intermediate and protein residues shorter than 4.0 Å are denoted by dashed lines. The DHAP is shown as a Fisher projection.

of the C-terminus, the structural changes upon substrate binding are restricted to side chain movements.

Schiff-Base Intermediate. The electron density in the active site clearly showed continuous electron density extending beyond Lys229, which forms the Schiff base with the substrate, indicating the formation of a covalent adduct (Figure 1). The shape of the electron density was consistent with the product Schiff base [N^6-(β-phosphoglyceryl)lysine] rather than the substrate Schiff base. Under steady-state conditions starting with Fru-1,6-P_2, most of the enzyme is bound to DHAP while 10−15% is bound to Fru-1,6-P_2 (*42*, *43*). The DHAP density contiguous with that of Lys229 is consistent with this observation. The covalently linked DHAP was observed in all four monomers.

The DHAP moiety makes a number of interactions within the active site. Figure 2 shows the schematic representation of phosphoglyceryl-linked lysine in the active site, including the length of hydrogen bonds between the DHAP moiety and protein residues. The C1-phosphate binding site is made of the main chain backbone nitrogens of Ser271, Gly272, Gly302, and Arg303, with somewhat closer contacts seen between the side chain hydroxyl of Ser271 and the guanidinium group of Arg303. The phosphoester oxygen O1 makes a hydrogen bond to the amide nitrogen of Gly302. The C3-hydroxyl of DHAP makes hydrogen bonds to the ϵ-amino group of Lys146 and side chain carboxyl group of Asp33. The ϵ-amino group of Lys229 makes hydrogen bonds to the carbonyl oxygen of Ser300. The residues identified as the C1-phosphate binding site in this structure show that it shares a common phosphate binding site with the noncovalent complexes of DHAP (*24*) or Fru-1,6-P_2 (*22*, *23*) with the exception of an additional ligand from Arg303. The involvement of Arg303 in C1-phosphate binding is remarkable since this residue has been shown to interact with the C6-phosphate moiety in the structure of the Fru-1,6-P_2 aldolase complex (*23*) and the C2-carbonyl oxygen of one of the DHAP molecules in the noncovalent DHAP−aldolase complex (*24*). A role for Arg303 as a "trigger" in the aldolase mechanism in relation to the C-terminal residues has been suggested (*22*), and the multiple conformations of this residue in the various liganded structures are consistent with this idea (see below).

Determinants of Specificity. The proximity of the Asp33 and Lys146 residues to C3 of the DHAP moiety has significance in the aldolase mechanism. Aldolase is specific with regard to the chirality at C3, only cleaving the carbon−carbon bond with the *S*-configuration (*14*) and stereospecifically protonating the enamine at the same position (*44*). L-Erythrulose 1-phosphate and D-xylulose 1,5-bisphosphate, both with the *S*-configuration at C3, are cleaved into DHAP and formaldehyde or glycoaldehyde, respectively (*45*, *46*). In contrast, D-erythrulose 1-phosphate and D-ribulose 1,5-bisphosphate, with the *R*-configuration at C3, are not cleaved but instead are slow-binding or competitive inhibitors (*47*). One of the determinants of stereospecificity at C3 observed in the structure may be the strictly conserved residue Ala31 (*48*). The Ala31 methyl carbon is positioned opposite the C3-hydroxyl group, 3.6 Å from C3, such that a sugar with the opposite stereochemistry would be sterically hindered.

In this model, the distances from Asp33 or Lys146 to C3 are 3.3 and 4.3 Å, respectively, with Asp33 on the pro-*S* hydrogen side and Lys146 on the pro-*R* hydrogen side. Furthermore, if the pro-*S* hydrogen at C3 of the DHAP moiety is replaced with C4 of Fru-1,6-P_2 (see Materials and Methods), the distances from C4 are 2.6 and 5.4 Å, respectively. In the model of Fru-1,6-P_2 based on the DHAP structure, the C4-hydroxyl group was located 2.3 Å from the carboxylate oxygen of Asp33 and 5.9 Å from the ϵ-amino group of Lys146, each of which has been proposed to be the catalytic base that initiates carbon−carbon bond cleavage (*19*, *20*). This makes Asp33 the more likely candidate for the proton abstraction from the C4-hydroxyl leading to C3−C4 bond cleavage.

The borohydride reaction has been shown to be stereospecific since, after acid hydrolysis of the protein, only N^6-(2-deoxy-2-glucitol) L-lysine (*S*-configuration at C2) was isolated between two possible products (*R*- or *S*-configuration at C2) (*30*). The structure of N^6-(β-phosphoglyceryl)lysine observed here is consistent with the *S*-configuration at C2 (*15*), indicating the hydride attacks the *re*-face of C2 of the Schiff base. It is likely that in forming the carbinolamine water attacks from the same side as that of the hydride in reducing the Schiff base (see below). In this case, the C2-hydroxyl of the carbinolamine points toward Glu187, which would be within hydrogen bonding distance. Glu187 is 4.0 Å from ϵ-amino group of Lys229 and is a conserved residue in all vertebrate aldolase sequences (*48*). The position of Glu187 in relation to the DHAP Schiff base, that is, near what would have been the C2-hydroxyl of carbinolamine in this structure, suggests a role in Schiff-base formation. In this position, Glu187 acts as a general acid to protonate the leaving hydroxyl group of the carbinolamine in the dehydration step, leading to Schiff-base formation.

Comparison with Noncovalently Bound Enzyme Complexes. As described earlier, there was no gross conformational change in the Schiff-base intermediate structure when compared to those of the native protein (*21*) or the noncovalent DHAP complexes (*24*). Thus, most of the changes reflect side chain movements. One interesting observation is the relative disposition of Arg303 and the C-terminus (Figure 3). In the structure reported here, the side chain of Arg303 moves into the active site cleft, making a hydrogen bond to the C1-phosphate oxygen (3.1 Å). In the published DHAP-bound structure [1ADO (*24*)], Arg303 makes a hydrogen bond with the C-terminus at Glu354 (2.8 Å), producing a "tucked in" conformation of the C-terminus. Glu354 was not observed in the structure reported herein due to the disorder of the C-terminus. Arg303 has been suggested to be a key functional residue in the substrate-induced conformational change from the K146A aldolase−Fru-1,6-P_2 complex structure (*22*). It is noteworthy that whenever the C-terminal portion of aldolase is ordered, as in the published crystal structure with DHAP (*24*), Arg303 interacts with the C-terminal residues and the C-terminal residues are tucked into the active site cleft. In contrast, when Arg303 makes hydrogen bonds to the α/β-barrel domain, as in our structure, the active site cleft is blocked by an Arg−X interaction and unavailable for the C-terminus, and thus the C-terminal residues are disordered. The coupled changes in the position of Arg303 and the C-terminal residues are shown in Figure 3. Arg303, by binding alternatively to the C6-phosphate (*22*) of the hexose sugar or the C1-phosphate of the product triose, may act as a trigger for the conformational change of the C-terminus. This C-terminal conformational change may be required for DHAP product release, which is likely the rate-limiting step in catalysis (*20*, *49*, *50*).

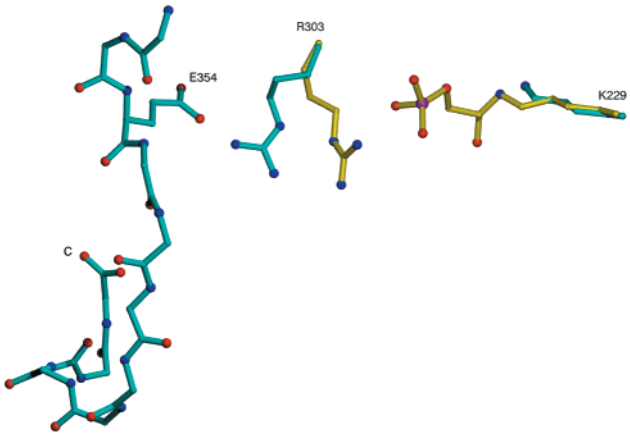

FIGURE 3: Alternative conformations of Arg303 in relation to the active site and the C-terminus. Superposition of the structures of Fru-1,6-P_2 aldolase noncovalently liganded to DHAP (1ADO, cyan) and covalently bound to reduced DHAP (1J4E, yellow). The trigger residue, Arg303, and Schiff-base-forming Lys229 are depicted for both structures. The side chains of the C-terminal residues (with the exception of Glu354) and the DHAP ligand are omitted from 1ADO for clarity. Note that the C-terminal residues of 1J4E are disordered and therefore not visible in the crystal structure. The C-terminus is labeled.

Relationship to Other Schiff-Base Aldolases. A number of enzymes catalyzing aldol cleavage and/or condensation belong to the class I aldolase family. Several enzymes have been studied by X-ray crystallography, and the three-dimensional structures of transaldolase, KDPG aldolase, *N*-acetylneuraminate lyase, and dihydropicolinate synthase are known (*25*, *51*−*53*). Among those enzymes, the half-reaction catalyzed by transaldolase is very similar to that of Fru-1,6-P_2 aldolase, as well as that of KDPG aldolase. Transaldolase catalyzes the reversible transfer of a dihydroxyacetone moiety, derived from fructose 6-phosphate, to erythrose 4-phosphate, forming sedoheptulose 7-phosphate and G3P (*54*). KDPG aldolase catalyzes the reversible cleavage of 2-keto-3-deoxyphosphogluconate to pyruvate and G3P. As in other enzymes in the class I aldolase family, the transaldolase reaction, and the KDPG aldolase reaction, proceed through the formation of a Schiff base between an active site lysine residue and the dihydroxyacetone or pyruvate moiety, respectively. The differences between KDPG aldolase and Fru-1,6-P_2 aldolase lie in substrate specificity for the C6-phosphate versus the C1-phosphate specificity for the linear sugar, but a very similar chemical mechanism can be drawn (*55*). The fundamental chemical differences between transaldolase and Fru-1,6-P_2 aldolase are that in transaldolase dihydroxyacetone does not dissociate from the enzyme after Schiff-base formation, but remains available for condensation with the aldehyde acceptor. Transaldolase and KDPG aldolase share the preference for C6-phosphohexoses. How do the structures of these enzymes compare? The structure of transaldolase B from *Escherichia coli* (*25*, *56*) exhibited a circular permutation in the protein sequence of the α/β-barrel. That is, the Schiff base-forming lysine of aldolase and transaldolase were aligned together so that the

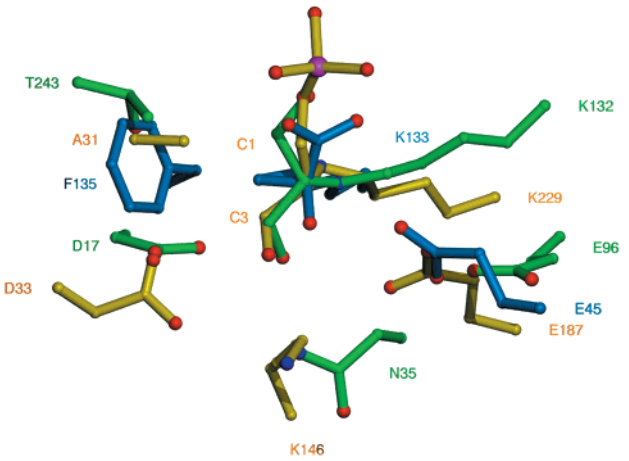

FIGURE 4: Superposition of the active site residues of Fru-1,6-P_2 aldolase, KDPG aldolase, and transaldolase. Fru-1,6-P_2 aldolase (1J4E), KDPG aldolase (1EUA), and transaldolase (1UCW) are shown as yellow, blue, and green ball-and-stick models, respectively. Residues within 5 Å of the catalytic lysine ϵ-amino group are shown.

first β-strand of transaldolase B can be overlaid with the third β-strand in the Fru-1,6-P_2 aldolase. No such permutation occurs in KDPG aldolase (*57*). The structure of transaldolase with the Schiff-base intermediate dihydroxyacetone was determined (*25*), and further similarity in the active site residues between aldolase and transaldolase was observed. However, the interpretation was difficult since there was no covalently bound intermediate available for Fru-1,6-P_2 aldolase. The aldolase Schiff-base structure determined here allows the comparison of the active sites of aldolase and transaldolase. Furthermore, the substrate-bound carbinolamine structure of KDPG aldolase allows overlay of this aldol cleavage enzyme with the other two. On the basis of the three-dimensional structure at the active site and amino acid comparison, three conserved residues from aldolase (Lys229, Glu187, and Asp33) can be overlaid with the conserved residues Lys132, Glu96, and Asp17 from transaldolase (*58*) and conserved residues Lys133 and Glu45 from KDPG aldolase (Figure 4). Both the aldolases and transaldolase Schiff-base intermediates exhibited the same configuration at C2 (when C1−C3 of DHAP, dihydroxyacetone, and pyruvate moiety from aldolase, transaldolase, and KDPG aldolase, respectively, were overlaid), suggesting that the catalytic lysine of each enzyme attacks the same face of their respective substrates. The positions of the essential catalytic dyad, Lys229-Glu187, were not much different between the enzymes with rms deviations of 1.4 Å for common atoms of aldolase and transaldolase, and 1.7 Å for common atoms of aldolase and KDPG aldolase. In transaldolase, Glu96 makes a hydrogen bond to a water molecule within hydrogen bonding distance of Lys132 instead of the direct hydrogen bond between Glu187 and Lys229 formed in Fru-1,6-P_2 aldolase and between Glu45 and Lys133 in KDPG aldolase. This alignment predicts that the Phe135 in KDPG aldolase plays the same role as Ala31 and Thr243 in aldolase and transaldolase, that of maintaining the stereospecificity at C3. This is consistent with the prediction based on the structure of the KDPG−pyruvate covalent complex (*26*).

One other difference in the active site structure between aldolase and transaldolase is the absence of a lysine residue corresponding to Lys146 in aldolase. Lys146 is substituted with Asn35 in transaldolase. If the role of Lys146 is to facilitate protonation of the carbanion to form the DHAP−

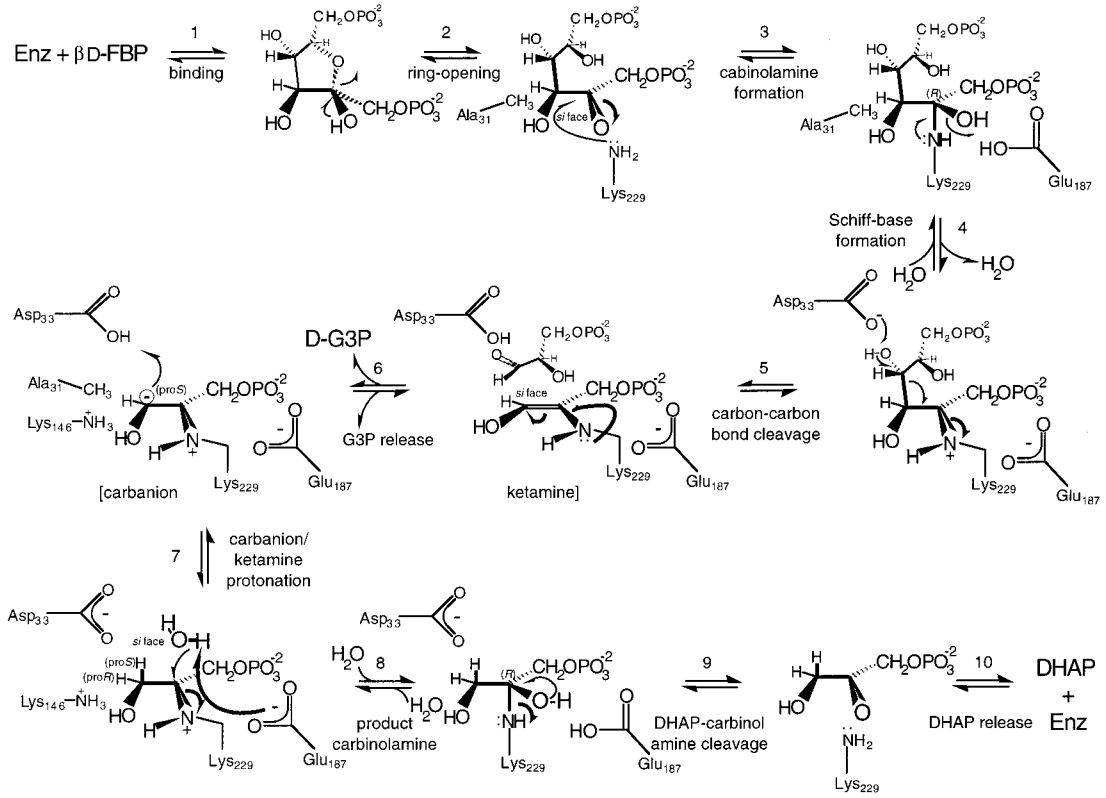

FIGURE 5: Proposed mechanism of Fru-1,6-P_2 aldolase based on the structure of the DHAP Schiff-base intermediate. Ten steps (numbered) for the reaction mechanism by aldolase are shown from hexose to triose. The residues provided by the enzyme are shown. Step 6 includes the ketimine/carbanion tautomerization in addition to G3P release.

Schiff-base intermediate that is subsequently released from the enzyme, there is no need for this residue to be conserved in transaldolase since dihydroxyacetone is not released. How Lys146 may facilitate protonation of the carbanion awaits further structural and mechanistic characterization.

Proposed Mechanism for Class I Aldolases. A common mechanism can be inferred from the conservation of active site geometry and functionality of Schiff-base aldolases described above (Figure 5). Following binding (step 1) and ring opening (step 2) (K. H. Choi and D. R. Tolan, personal communication), covalent catalysis is initiated by *si*-face attack by the ϵ-amino group (Lys229 for aldolase) on the C2-carbonyl (*15*) to form the (2*R*)-carbinolamine. The dehydration of the carbinolamine to form the imine, or hydrolysis in the reverse direction (step 4), is acid-catalyzed by the adjacent Glu residues (Glu187 for aldolase, Glu96 for transaldolase, and Glu45 for KDPG aldolase). The C2-hydroxyl is protonated to leave as water, or is deprotonated for *re*-face attack of the imine in the reverse reaction (*30*). This is on the same side as the hydride reduction of the imine, as was inferred biochemically (*30*) and is confirmed here. The *si*-face of the imine is not available to solvent. Attack at the *si*-face, which is the direction taken by the Lys, is sterically hindered by enzymic residues in the active site, leaving only the *re*-face exposed to solvent. The electron sink formed at C2 makes facile the proton abstraction at C4-hydroxyl by an Asp residue acting as a base (Asp33 in aldolase and Asp17 in transaldolase). This leads to subsequent C3−C4 bond cleavage (step 5). After carbon−carbon bond cleavage, G3P, the first product, is released (*14*), and a carbanion/enamine is formed at the active site (step 6) (*12*). The protonated Asp33 donates a *si*-face proton to the resulting carbanion to form the product imine (step 7). The protonation is to the same bond on C3 formerly to C4 (*14*, *44*). This step may be facilitated by the proximity of Lys146 (4.3 Å), although the mechanism of this activity is unknown. For aldolases, the importance of conserved residues Asp33 and Lys146 in the catalytic cycle has been established by site-directed mutagenesis (*19*, *20*, *50*). Asp33 mutant enzymes (D33A and D33S) have drastically reduced k_{cat} values (3600−5600-fold decrease) and low carbanion/enamine intermediate levels, as measured by the extent of carbanion oxidation (*19*). The D33A mutant exhibited 17−29-fold lower levels of carbanion intermediate from Fru-1,6-P_2 than from DHAP (*19*), which is consistent with the role of Asp33 in C3−C4 bond cleavage since carbon bond cleavage is not required to generate the carbanion in DHAP. Furthermore, transient-state kinetics revealed that carbon−carbon bond cleavage is rate-limiting in these enzymes (*59*). Lys146 mutant enzymes (K146A, K146Q, K146L, K146H, and K146R) have been generated by site-directed mutagenesis (*20*, *50*). The Lys146 mutants form a Schiff base with Fru-1,6-P_2; however, the K146A, K146Q, and K146L mutant enzymes were unable to cleave the carbon bond, since no triose product was detectable with Fru-1,6-P_2 as the substrate. K146H restores some activity at pH <8.5 (but not above), and the rate of carbon−carbon bond cleavage at pH 7.4 was measurable albeit low (3000-fold decrease) (*20*). If a positive charge is what is required for effective catalysis, then H146 has an increased pK_a (∼8.5) relative to that of His in solution. The need for a positive charge is further supported by the kinetics of the K146R mutant enzyme, which is only 200-fold decreased in activity and has the same pH−rate profile as the wild type (*50*). As described above, the importance of a positive charge at position 146 in aldolase versus transaldolase may be an important catalytic determinant. The hydrolysis and release of the second product, DHAP (steps 8−10), in aldolase are essentially the reverse of steps 4, 3, and 1. The rate-limiting step in the wild-type aldolase is step 10, and the role of the conformational change in the C-terminus is likely critical in this process (*23*, *36*, *46*).

ACKNOWLEDGMENT

We thank Dr. Herb Kagen for critical and thoughtful comments on the manuscript.

REFERENCES

1. Rutter, W. J. (1960) *Enzymes 5*, 341−372.
2. Creighton, D. J., and Murthy, N. S. R. K. (1990) *Enzymes 19*, 323−421.
3. Penhoet, E. E., Rajkuman, R., and Rutter, W. J. (1966) *Proc. Natl. Acad. Sci. U.S.A. 56*, 1275−1282.
4. Baron, C. B., Ozaki, S., Watanabe, Y., Hirata, M., LaBelle, E. F., and Coburn, R. F. (1995) *J. Biol. Chem. 270*, 20459−20465.
5. Penhoet, E. E., and Rutter, W. J. (1971) *J. Biol. Chem. 246*, 318−323.
6. Walker, P. R., and Potter, V. R. (1972) *Adv. Enzymol. Regul. 10*, 339−364.
7. Matsushima, T., Kawabe, S., Shibuya, M., and Sugimura, T. (1968) *Biochem. Biophys. Res. Commun. 30*, 565−570.
8. Tolan, D. R. (1995) *Hum. Mutat. 6*, 210−218.
9. Izzo, P., Costanzo, P., Lupo, A., Rippa, E., Borghese, A. M., Paolella, G., and Salvatore, F. (1987) *Eur. J. Biochem. 164*, 9−13.
10. Tolan, D. R., Amsden, A. B., Putney, S. D., Urdea, M. S., and Penhoet, E. E. (1984) *J. Biol. Chem. 259*, 1127−1131.
11. Grazi, E., Rowley, P. T., Chang, T., Tchola, O., and Horecker, B. L. (1962) *Biochem. Biophys. Res. Commun. 9*, 38−43.
12. Christen, P., and Riordan, J. F. (1968) *Biochemistry 7*, 1531−1538.
13. Allen, K. N. (1998) in *Comprehensive Biological Catalysis* (Sinnott, M., Ed.) pp 135−172, Academic Press, New York.
14. Rose, I. A., O'Connell, E. L., and Mehler, A. H. (1965) *J. Biol. Chem. 240*, 1758−1765.
15. di Iasio, A., Trombetta, G., and Grazi, E. (1977) *FEBS Lett. 73*, 244−246.
16. Healy, M. J., and Christen, P. (1973) *Biochemistry 12*, 35−41.
17. Lai, C. Y., and Oshima, T. (1971) *Arch. Biochem. Biophys. 144*, 363−374.
18. Littlechild, J., and Watson, H. (1993) *Trends Biochem. Sci. 18*, 36−39.
19. Morris, A. J., and Tolan, D. R. (1993) *J. Biol. Chem. 268*, 1095−1100.
20. Morris, A. J., and Tolan, D. R. (1994) *Biochemistry 33*, 12291−12297.
21. Sygusch, J., Beaudry, D., and Allaire, M. (1987) *Proc. Natl. Acad. Sci. U.S.A. 84*, 7846−7850.
22. Choi, K. H., Mazurkie, A. S., Morris, A. J., Utheza, D., Tolan, D. R., and Allen, K. N. (1999) *Biochemistry 38*, 12655−12664.
23. Dalby, A., Dauter, Z., and Littlechild, J. A. (1999) *Protein Sci. 8*, 291−297.
24. Blom, N., and Sygusch, J. (1997) *Nat. Struct. Biol. 4*, 36−39.
25. Jia, J., Schorken, U., Lindqvist, Y., Sprenger, G. A., and Schneider, G. (1997) *Protein Sci. 6*, 119−124.
26. Allard, J., Grochulski, P., and Sygusch, J. (2001) *Proc. Natl. Acad. Sci. U.S.A. 98*, 3679−3684.
27. Ling, M. M., and Robinson, B. H. (1997) *Anal. Biochem. 254*, 157−178.
28. Baranowski, T., and Niederland, T. R. (1949) *J. Biol. Chem. 180*, 543−551.
29. Racker, E. (1952) *J. Biol. Chem. 196*, 347−351.

30. Trombetta, G., Balboni, G., di Iasio, A., and Grazi, E. (1977) *Biochem. Biophys. Res. Commun. 74*, 1297−1301.
31. Otwinowski, Z., and Minor, W. (1997) *Methods Enzymol. 276*, 307−326.
32. Matthews, B. W. (1985) *Methods Enzymol. 114*, 176−187.
33. Brünger, A. T., Adams, P. D., Clore, G. M., DeLano, W. L., Gros, P., Grosse-Kunstleve, R. W., Jiang, J.-S., Kuszewski, J., Nilges, M., Pannu, N. S., Read, R. J., Rice, L. M., Simonson, T., and Warren, G. L. (1998) *Acta Cryst. D54*, 905−921.
34. Collaborative Computational Project Number 4 (1994) *Acta Crystallogr. D50*, 760−763.
35. Jones, T. A., Zou, J. Y., Cowan, S. W., and Kjeldgaard, M. (1991) *Acta Crystallogr. A47*, 110−119.
36. Berthiaume, L., Tolan, D. R., and Sygusch, J. (1993) *J. Biol. Chem. 268*, 10826−10835.
37. Hartman, F. C., and Brown, J. P. (1976) *J. Biol. Chem. 251*, 3057−3062.
38. Dreschler, E. R., Boyer, P. D., and Kowalsky, A. G. (1959) *J. Biol. Chem. 234*, 2627−2634.
39. Berthiaume, L., Loisel, T. P., and Sygusch, J. (1991) *J. Biol. Chem. 266*, 17099−17105.
40. Rose, I. A., and O'Connell, E. L. (1969) *J. Biol. Chem. 244*, 126−134.
41. Gamblin, S. J., Davies, G. J., Grimes, J. M., Jackson, R. M., Littlechild, J. A., and Watson, H. C. (1991) *J. Mol. Biol. 219*, 573−576.
42. Avigad, G., and England, S. (1972) *Arch. Biochem. Biophys. 153*, 337−346.
43. Rose, I. A., and O'Connell, E. L. (1977) *J. Biol. Chem. 252*, 479−482.
44. Rose, I. A., and Rieder, S. V. (1958) *J. Biol. Chem. 231*, 315−329.
45. Gillett, J. W., and Ballou, C. E. (1963) *Biochemistry 2*, 547−552.
46. Mehler, A. H., and Cusic, M. E., Jr. (1967) *Science 155*, 1101−1103.
47. Blonski, C., Gefflaut, T., and Perie, J. (1995) *Bioorg. Med. Chem. 3*, 1247−1253.
48. Berardini, T. Z. R. (1998) Ph.D. Dissertation, Boston University, Boston, MA.
49. Rose, I. A., Warms, J. V. B., and Kuo, D. J. (1987) *J. Biol. Chem. 262*, 692−701.
50. Morris, A. J., Davenport, R. C., and Tolan, D. R. (1996) *Protein Eng. 9*, 61−67.
51. Mirwaldt, C., Korndorfer, I., and Huber, R. (1995) *J. Mol. Biol. 246*, 227−239.
52. Izard, T., Lawrence, M. C., Malby, R. L., Lilley, G. G., and Colman, P. M. (1994) *Structure 2*, 361−369.
53. Mavridis, I. M., Hatada, M. H., Tulinsky, A., and Lebioda, L. (1982) *J. Mol. Biol. 162*, 419−444.
54. Tsolas, O., and Horecker, B. (1972) *Enzymes 7*, 259−280.
55. Vlahos, C. J., and Dekker, E. E. (1990) *J. Biol. Chem. 265*, 20384−20389.
56. Jia, J., Huang, W., Schorken, U., Sahm, H., Sprenger, G. A., Lindqvist, Y., and Schneider, G. (1996) *Structure 4*, 715−724.
57. Pouyssegur, J., and Stoeber, F. (1972) *Mol. Gen. Genet. 114*, 305−311.
58. Schorken, U., Thorell, S., Schurmann, M., Jia, J., Sprenger, G. A., and Schneider, G. (2001) *Eur. J. Biochem. 268*, 2408−2415.
59. Morris, A. J. (1995) Ph.D. Dissertation, Boston University, Boston, MA.
60. Kraulis, P. J. (1991) *J. Appl. Crystallogr. 24*, 946−950.

BI0114877